

Particle Deposition onto Solid Surfaces with Micropatterned Charge Heterogeneity: The “Hydrodynamic Bump” Effect

Menachem Elimelech,* Jeffrey Y. Chen, and Zachary A. Kuznar

Department of Chemical Engineering, Environmental Engineering Program, Yale University, P.O. Box 208286, New Haven, Connecticut 06520-8286

Received March 25, 2003. In Final Form: June 14, 2003

A radial stagnation-point flow cell utilizing an optical microscope and an image-capturing device was used to directly observe the deposition kinetics of colloidal particles onto micropatterned glass surfaces with well-defined surface charge features. Surface charge heterogeneity was microfabricated onto glass surfaces by silanizing specified regions of the glass surface by a soft lithographic technique. At a certain combination of solution ionic strengths and particle Peclet numbers, the observed deposition rates deviated from predictions on the basis of a particle-deposition model for surfaces with macroscopic patchwise charge heterogeneity. The results are attributed to the interplay between hydrodynamic and electrostatic double-layer interactions and are explained by a phenomenon we term the “hydrodynamic bump” effect.

Introduction

Solid surfaces in technological and natural systems are often chemically heterogeneous. Some of the sources of chemical heterogeneity include differences in constituent minerals, chemical imperfections, and surface-bound “impurities” and coatings.^{1–3} This chemical variability results in an uneven or heterogeneous surface charge distribution at various length scales.^{4–11} Direct and indirect observations provide ample evidence for the presence of macroscopic and microscopic charge heterogeneities on solid surfaces.^{1,3,4}

Surfaces with a macroscopic charge heterogeneity have been effectively modeled as a patchwork mosaic with individual patches treated as isolated homogeneous entities having a uniform surface charge.^{12–14} These patches are assumed to be much larger than the interacting colloidal particles such that the interactions between patch boundaries have a negligible effect on particle deposition. For such surfaces, particle deposition is considered to be a linear combination of depositions on the various surface patches and regions.¹³ Microscopic-scale surface charge heterogeneity, on the other hand, is much less understood and is relatively unexplored.^{6,7,11} The lack of systematic experimental studies on microscopic surface charge het-

erogeneity is attributed to the difficulties in generating well-controlled microscopic-scale surface heterogeneities.

Latest advances in soft lithographic techniques have enabled the fabrication of microscopic surface features on solid, flat surfaces.^{15,16} We have recently extended such techniques to micropattern surface charge heterogeneity on glass surfaces by the chemical modification of specified surface regions with aminosilane.¹⁷ The resulting micropatterned surfaces can be well-suited for fundamental investigations on the influence of microscopic charge heterogeneity on the interaction between colloidal particles and heterogeneous surfaces.

In this paper, we use micropatterned glass surfaces and a stagnation-point flow (SPF) system to investigate the influence of microscopic charge heterogeneity on colloid deposition behavior under dynamic flow conditions. In particular, we investigate the validity of the macroscopic patch model for surfaces where the heterogeneously charged patches are not *much* larger than the particle size (i.e., same order of magnitude). We demonstrate that the patch model for particle deposition breaks down under certain physicochemical conditions because of a phenomenon we term the “hydrodynamic bump” effect. This phenomenon is attributed to the coupling between hydrodynamic and electrostatic double-layer interactions. The departure from the patch model is directly related to the particle Peclet number and the solution ionic strength.

Materials and Methods

Elastomeric Stamp. Surface charge heterogeneity was micropatterned onto microscope cover glass slides by silanizing well-controlled regions of the glass surface. Micropatterns were produced by an elastomeric stamp, cast from a microlithographically patterned master mold chip. The master mold is a 5 × 5 mm oxidized silicon chip patterned via electron-beam lithography. The chip has rectangular channels, 5- μ m wide and 0.5- μ m deep, spaced 5- μ m apart and extending the entire 5-mm length of the chip. Poly(dimethylsiloxane) (PDMS) (Sylgard 184 Silicone Elastomer Kit, Dow Corning, Midland, MI) was used to make the elastomeric patterned stamp.

Micropatterning Surface Charge Heterogeneity. Prior to micropatterning, the microscope cover glass slides were cleaned by soaking in 4 M HCl for 24 h, then rinsing with 1 M NaOH for 15 min, followed by a deionized water rinse. Aminoethylami-

* Corresponding author.

- (1) Ryan, J. N.; Elimelech, M. *Colloids Surf., A* **1996**, *107*, 1.
- (2) Hiemstra, T.; van Riemsdijk, W. H.; Bolt, G. H. *J. Colloid Interface Sci.* **1989**, *133*, 105.
- (3) Walz, J. Y. *Adv. Colloid Interface Sci.* **1998**, *74*, 119.
- (4) Vreeker, R.; Kuin, A. J.; Den Boer, D. C.; Hoekstra, L. L.; Agterof, W. G. M. *J. Colloid Interface Sci.* **1992**, *154*, 138.
- (5) Grant, M. L.; Saville, D. A. *J. Colloid Interface Sci.* **1995**, *171*, 35.
- (6) Miklavic, S. J.; Chan, D. Y. C.; White, L. R.; Healy, T. W. *J. Phys. Chem.* **1994**, *98*, 9022.
- (7) Sader, J. E.; Gunning, J. S.; Chan, D. Y. C. *J. Colloid Interface Sci.* **1996**, *182*, 516.
- (8) Richmond, P. *J. Chem. Soc., Faraday Trans. 2* **1974**, *8*, 1066.
- (9) Kuin, A. *J. Faraday Discuss. Chem. Soc.* **1990**, *90*, 235.
- (10) Schuhmann, D.; Bertrand, D. *J. Colloid Interface Sci.* **1987**, *116*, 159.
- (11) Khachatourian, A. V. M.; Wistrom, A. O. *J. Phys. Chem. B* **1998**, *102*, 2483.
- (12) Koopal, L. K.; Dukhin, S. S. *Colloid Surf., A* **1993**, *73*, 201.
- (13) Song, L. F.; Johnson, P. R.; Elimelech, M. *Environ. Sci. Technol.* **1994**, *28*, 1164.
- (14) Elimelech, M.; Gregory, J.; Jia, X.; Williams, R. *Particle Deposition & Aggregation. Measurement, Modeling and Simulation*; Butterworth-Heinemann: Oxford, U.K., 1995.

(15) Xia, Y.; Whitesides, G. M. *Annu. Rev. Mater. Sci.* **1998**, *28*, 153.

(16) Kim, E.; Xia, Y.; Whitesides, G. M. *Adv. Mater.* **1996**, *8*, 245.

(17) Chen, J. Y.; Klemic, J. F.; Elimelech, M. *Nano Lett.* **2002**, *2*, 393.

nomethylphenethyltrimethoxysilane (Gelest, Inc., Tullytown, PA) was used as the silanizing agent because of its enhanced hydrolytic stability compared to other triethoxy derivatives.^{17,18} A small volume (10 μL) of the aminosilane [0.2% (w/w) stock solution] was placed on the glass surface, followed by firmly pressing the PDMS mold with the patterned relief structure against the glass substrate. Pressing the mold expelled the aminosilane between the mold and the glass surface where contact was made, thus creating a rectangular pattern of aminosilane stripes on the glass surface in the mold's channels. The glass was then cured under vacuum conditions at 80 °C for 30 min and later without a vacuum at 130 °C for 90 min. Subsequent removal of the PDMS mold resulted in a surface with 5- μm -wide silanized micropatterns spaced 5- μm apart. We have shown elsewhere via streaming potential measurements that the amino-silanized glass surface is positively charged at the pH range used for the deposition experiments (pH 5.6–5.8).¹⁹ We further showed that, for glass surfaces where the aminosilane was expelled by the PDMS mold in the manner described above, the presence of minute impurities of aminosilane does not alter the ζ potential because such surfaces still have a negative ζ potential. Thus, for our deposition experiments with positively charged amidine latex particles, such glass surfaces are favorable for deposition (i.e., the interaction force between the particle and the glass surface is attractive).

It is also worthwhile to note that, after curing, the aminosilane layer formed in the rectangular channels of the PDMS mold does not significantly change the topography of the glass surface. Atomic force microscopy imaging of the micropatterns revealed that the thickness of the silanized layer midway at the channel is not different than that of the glass surface, but at the edges of the channel, the thickness increases to about 4 nm. Because the particle-deposition experiments are carried out with 2.1- μm particles, we expect such morphological heterogeneities to have a negligible effect on the particle-deposition behavior.

Colloidal Particles. Polystyrene latex particles with amidine functional groups (Interfacial Dynamics Corp., Portland, OR) were used as model colloidal particles for the deposition experiments. The monodispersed particles had a mean diameter of 2.1 μm (coefficient of variation of 3.2%) and a surface charge density of 30.2 $\mu\text{C}/\text{cm}^2$. As a result of the amidine functional groups, the particles had a positive surface charge at the pH range used in the deposition experiments (pH 5.6–5.8). The latex particle ζ potentials calculated from the measured electrophoretic mobilities (ZetaPALS, Brookhaven Instruments, Inc.) at pH 5.7 and ionic strengths of 10^{-3.5}, 10^{-3.0}, and 10^{-2.5} M KCl (as was used in the particle-deposition experiments) were 71.6, 55.9, and 41.2 mV, respectively.

SPF System. A radial SPF system was utilized for the particle-deposition experiments. The colloidal suspension was pumped by a syringe pump (model 230, KD Scientific) into a custom-made glass cell through a 2-mm inner diameter capillary tube. Upon emerging from the capillary, the suspension impinged against the transparent microscope cover glass located 2-mm from the capillary opening. The colloidal suspension was continuously removed from the cell via a waste stream. Particle deposition onto the glass surface was observed in real time from above by an optical microscope (Axioplan 2, Zeiss, Thornwood, NY). A charge-coupled device (CCD) camera (CCD-300-IFG, Dage MTI, Michigan City, IN) recorded the images in an area of 80 \times 106 μm around the stagnation point. The images were later analyzed with image-analysis software (KS400, Zeiss, Thornwood, NY).

Particle-Deposition Experiments. Particle-deposition experiments were carried out with the 2.1- μm amidine latex particles (60 mg/L or 1.173 \times 10⁷ cm⁻³) in electrolyte solutions of 10^{-2.5}, 10^{-3.0}, and 10^{-3.5} M KCl. Flow rates varied from 3 to 11 mL/min, corresponding to particle Peclet numbers in the range of 1.15–10.52 and Reynolds numbers in the range of 15.9–58.4. Experiments were carried out at room temperature (24 \pm 1 °C) and a fixed pH (ca. 5.7).

Utilizing the CCD camera, images of particle deposition in a 80 \times 106 μm area at the stagnation-point region were captured every 1 min. The images were analyzed to determine the particle-deposition flux (number of particles per area per time). Results are expressed in terms of the dimensionless Sherwood number:

$$Sh = \frac{J a_p}{C_0 D_\infty} \quad (1)$$

where J is the particle-deposition flux, a_p is the particle radius, C_0 is the bulk number concentration of the particles, and D_∞ is the bulk diffusion coefficient calculated from the Stokes–Einstein equation. The experimental deposition flux, J , was determined from the initial slope of the measured number of deposited particles as a function of time in the stagnation-point region. Equation 1 was then used to express the particle-deposition rate in terms of the Sherwood number, Sh .

Results and Discussion

Particle Deposition onto Micropatterned Glass.

Particle-deposition rates on the micropatterned glass surfaces were investigated as a function of solution ionic strength (KCl) and flow rate. Variations in the flow rates resulted in corresponding variations of the particle Peclet number and the SPF capillary Reynolds number. For our SPF system, these dimensionless numbers are defined as^{14,20}

$$Pe = \frac{v_r a_p}{D_\infty} \quad (2)$$

$$Re = \frac{\rho V_0 R}{\mu} \quad (3)$$

where v_r is a characteristic radial flow velocity, a_p is the particle radius (1.05 μm), D_∞ is the bulk diffusion coefficient, ρ is the fluid density, V_0 is the average velocity in the capillary (flow rate divided by capillary cross-sectional area), R is the radius of the capillary (1.0 mm), and μ is the viscosity of the aqueous solution. The characteristic radial velocity v_r is calculated at a radial position $r = a_p$ and a separation distance $z = a_p$.^{14,20}

$$v_r = \frac{\alpha V_0}{R^2} r z = \frac{\alpha V_0}{R^2} a_p^2 \quad (4)$$

where α is a parameter depending on the Reynolds number and the geometry of the system (i.e., capillary radius and the separation distance between the capillary opening and the microscope cover glass).²⁰

To further analyze particle deposition onto surfaces with microscopic charge heterogeneity, we compared the deposition rate onto the micropatterned glass surfaces to the deposition rate based on the patch model for particle deposition onto heterogeneously charged surfaces. The latter was determined experimentally as follows. At a given flow rate and KCl concentration, the Sherwood number was first determined for completely “favorable” deposition (i.e., deposition onto a clean glass slide where attractive double-layer interactions predominate). Using eq 1 and the procedure described earlier, we can determine the Sherwood number for “favorable” surfaces, Sh_f , for the given physicochemical conditions (KCl concentration and flow rate). Similarly, we determine the “unfavorable” deposition (i.e., deposition onto a completely silanized glass slide where repulsive double-layer interactions predomi-

(18) Arkles, B.; Anderson, R.; Larson, G. L.; Smith, C. *Silicon Compounds Register and Review*, 5th ed.; United Chemical Technologies: Bristol, U.K., 1991.

(19) Walker, S. L.; Bhattacharjee, S.; Hoek, E. M. V.; Elimelech, M. *Langmuir* **2002**, *18*, 2193.

(20) Dabros, T.; van de Ven, T. G. M. *Colloid Polym. Sci.* **1983**, *261*, 694.

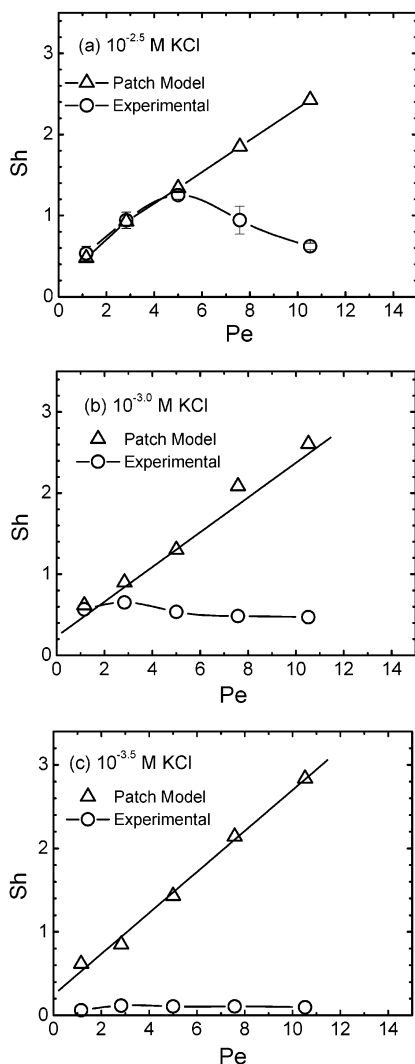


Figure 1. Variation of the particle-deposition rate (expressed as the Sherwood number) with the particle Peclet number for particle deposition at various ionic strengths: (a) $10^{-2.5}$, (b) $10^{-3.0}$, and (c) $10^{-3.5}$ M KCl. The particle diameter was fixed ($2.1 \mu\text{m}$) during the experiments, and the particle Peclet number was varied by changing the flow rate in the SPF system. The solution pH during the deposition experiments was fixed at approximately 5.7.

nate) and express it in terms of Sh_u . Utilizing the patch model for which the overall particle-deposition rate is a linear combination of the favorable and unfavorable deposition rates, the predicted Sherwood number for the patch model follows:^{13,14}

$$Sh_{\text{patch}} = \lambda Sh_f + (1 - \lambda) Sh_u \quad (5)$$

where λ is the fraction of favorable patches (i.e., surface regions where particle deposition is “favorable”). For our system of positively charged latex particles and micropatterned glass surfaces, $\lambda = 0.5$ because the $5\text{-}\mu\text{m}$ -wide aminosilane-modified stripes alternate with the $5\text{-}\mu\text{m}$ -wide bare glass stripes.

Figure 1 presents the particle-deposition rate (expressed in terms of the Sherwood number) as a function of the particle Peclet number for experiments at $10^{-2.5}$, $10^{-3.0}$, and $10^{-3.5}$ M KCl. The particle Peclet numbers ranged from 1.15 (corresponding to a flow rate of 3.00 mL/min or a Reynolds number of 15.9) to 10.52 (corresponding to a flow rate of 11.00 mL/min or a Reynolds number of 58.4). As was observed, deposition rates based on the patch model

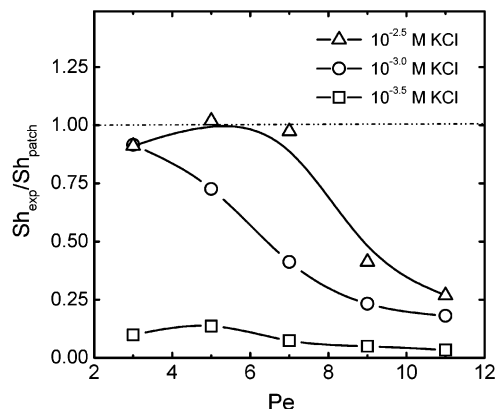


Figure 2. Variation of the relative deposition rate, that is, the measured Sherwood number divided by the Sherwood number predicted for the patch model, as a function of the particle Peclet number for the particle-deposition runs shown in Figure 1. Experimental conditions are given in Figure 1. Note that a value of $Sh_{\text{exp}}/Sh_{\text{patch}} = 1$ corresponds to a perfect match between the experimental results and the patch-model predictions.

(open triangles) increase linearly with the Peclet number because of the increased particle transfer rate at higher flow rates. The deposition rate onto the micropatterned glass surfaces, however, deviates significantly from the patch model. It is clearly observed that the deposition rate onto the micropatterned glass surfaces approaches the predictions based on the patch model only at low Peclet numbers and a moderate ionic strength. Indeed, at the lowest ionic strength ($10^{-3.5}$ M KCl), the particle-deposition rate on the micropatterned surface is negligible and does not approach the value expected based on the patch model for the employed experimental conditions.

It is worthwhile to mention that, for our system, $Sh_f \gg Sh_u$ at the lowest ionic strength used ($10^{-3.5}$ M KCl). At the higher ionic strengths, particle deposition was also observed on the “unfavorable”, silanized regions, but it was always small compared to deposition onto the “favorable” surface regions. The deposition of the amidine latex particles on the unfavorable (silanized) regions may be attributed to chemical heterogeneities or hydrophobic interactions between the latex particles and the aminosilane layer.

Deviation from the Patch Model. The above results point out that (1) deviation from the patch model occurs at high flow rates (or Peclet numbers), (2) the patch model approximates the deposition rate at lower Peclet numbers, and (3) deviation from the patch-model predictions occurs at a lower Peclet number for the lower-ionic-strength runs. To further illustrate the deviation from the patch model, Figure 2 presents the data by plotting the experimental Sherwood number scaled with the patch-model prediction ($Sh_{\text{exp}}/Sh_{\text{patch}}$) versus the Peclet number for the three ionic strengths ($10^{-2.5}$, $10^{-3.0}$, and $10^{-3.5}$ M KCl). Note that $Sh_{\text{exp}}/Sh_{\text{patch}} = 1$ corresponds to a perfect match between the experimental results and the patch-model predictions. Figure 2 confirms our earlier observation that deviation from the patch-model behavior occurs at a lower value of the Peclet number for a lower-ionic-strength solution (or a larger Debye screening length, κ^{-1}). The results point to a coupling between hydrodynamic interactions (represented by the Peclet number) and electrostatic double-layer interactions (controlled by ionic strength). As we will show in the next subsection, this interplay between hydrodynamic and electrostatic double-layer interactions dictates the observed particle-deposition behavior onto the micropatterned, heterogeneously charged glass surface.

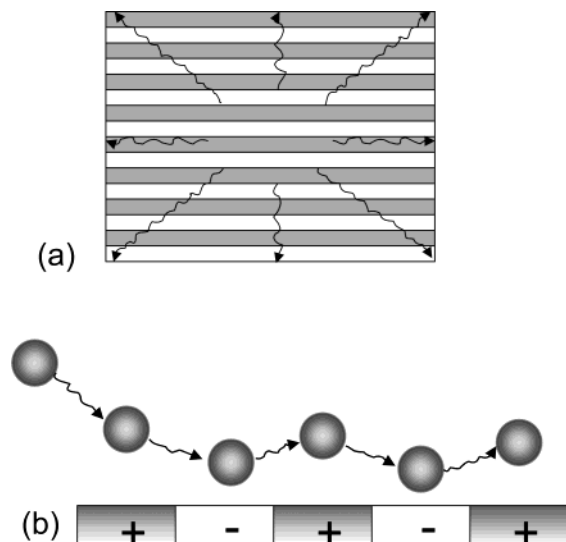


Figure 3. Schematic illustration of the “hydrodynamic bump” effect. (a) Plane view of the radial flow over the micropatterned glass surface in the SPF region where particle deposition is observed. (b) Side view of the “hydrodynamic bump” effect and the resulting trajectory of a particle flowing over the chemically heterogeneous micropatterns. The shaded regions represent the aminosilanzed (positively charged) stripes, and the clear regions represent the bare (negatively charged) glass stripes. The particles are positively charged.

Breakdown of the Patch Model—The “Hydrodynamic Bump” Effect. The salient deviation from the patch model, as is seen from the results in Figures 1 and 2, is somewhat surprising considering the feature size of the patchwise charge heterogeneity ($5\ \mu\text{m}$) is larger than the particle size. Our results further demonstrate that the deviation from the patch model is more pronounced when decreasing the solution ionic strength and increasing the flow rate. We propose that the particle-deposition behavior onto the micropatterned glass surface is determined by a unique interplay between hydrodynamic and electrostatic double-layer interactions. For our micropatterned surface, these interactions are controlled by the flow intensity, particle size, and solution ionic strength. Their combined effect on the deposition behavior and the deviation from the patch model is explained by the so-called “hydrodynamic bump” effect, as is described schematically in Figure 3.

The flow in the stagnation-point region has both normal and tangential or radial components.^{14,21} Particles flowing over the micropatterns will experience repulsive electrostatic double-layer forces when moving over the silanized regions (both are positively charged) and attractive electrostatic double-layer forces when flowing over the

bare glass regions (the particle and glass surface are oppositely charged). When a particle is moving laterally across a similarly charged (unfavorable) surface stripe toward the oppositely charged (favorable) surface stripe (Figure 3a), the tangential, or shear, component of the fluid flow creates a zone on the downgradient favorable stripe where the probability of subsequent deposition is reduced by the combined effect of hydrodynamic and electrostatic double-layer interactions. For a given ionic strength, the fraction of this excluded region increases as the particle size and the approach velocity increase (as characterized by a larger Peclet number). Smaller particles and lower approach velocities (i.e., lower Peclet numbers) result in more efficient diffusive transport and, hence, a smaller excluded region for favorable deposition. At sufficiently small Peclet numbers, the excluded region is negligible, and the particle-deposition rate approaches the patch-model predictions, as we have seen in Figures 1 and 2. The reduced deposition region is also influenced by the solution ionic strength as a result of electrostatic double-layer repulsion between the unfavorable region and the approaching particles, with lower ionic strengths resulting in an extended excluded zone on the favorable stripe for a given approach velocity. Thus, the interplay between hydrodynamic interactions (characterized by the particle Peclet number) and electrostatic double-layer interactions (controlled by the solution ionic strength) can explain the observed deposition behavior and the breakdown of the patch model for particle deposition onto patchwise, chemically heterogeneous surfaces.

Conclusion

Chemically micropatterned glass surfaces can be effectively used to investigate the interaction between colloidal particles and solid surfaces with microscopic surface charge heterogeneity. For surfaces having microscopic surface charge heterogeneity with feature sizes larger than the interacting particles, the deposition behavior cannot be solely explained by the macroscopic patch model. For a given microscopically heterogeneous surface, colloid deposition kinetics can be described well by the patch model for low Peclet numbers and moderate-to high-ionic-strength conditions. However, significant deviations from the patch-model behavior are observed for high Peclet numbers and/or low ionic strength conditions. This phenomenon can be explained by the “hydrodynamic bump” effect and is attributable to the interplay between hydrodynamic and electrostatic double-layer interactions.

Acknowledgment. Research was supported by the National Science Foundation, Grant CHE-0089156, under Collaborative Research Activities in Environmental Molecular Science (CRAEMS).

LA034516I

(21) Adamczyk, Z.; Warszynski, P.; Szyk-Warszynska, L.; Weronki, P. *Colloids Surf., A* **2000**, *165*, 157.